

1. 33 p.
MTP-TEST-63-4

March 12, 1963

64

CODE-2B

1/CA(2)
GEORGE C. MARSHALL

**SPACE
FLIGHT
CENTER**

6621703

HUNTSVILLE, ALABAMA

(NASA TMX 50557)
MTP-TEST-63-4)

Full
PERFORMANCE CHARACTERISTICS OF A LARGE FREE-FIELD
EXPONENTIAL HORN

By

Richard N. Tedrick

(NASA-TM-X-50557) PERFORMANCE
CHARACTERISTICS OF A LARGE
FREE-FIELD EXPONENTIAL HORN (NASA)
33 p

1 ref
N94-71199

Unclass

29/71 0202215



CASE FILE COPY

GEORGE C. MARSHALL SPACE FLIGHT CENTER

MTP-TEST-63-4

PERFORMANCE CHARACTERISTICS OF A LARGE FREE-FIELD
EXPONENTIAL HORN

By

Richard N. Tedrick

ABSTRACT

15425

This report presents the characteristics of a large electro-pneumatic transducer and exponential horn system which was installed at Marshall Space Flight Center to simulate the rocket engine noise produced during a static test. The output of the system was found experimentally to be about 24 decibels lower than the SATURN S-I static tests.

Performance characteristics are presented showing the frequency response of the horn as a mechanical coupler into the atmosphere. The electrical, electronic and pneumatic control systems are explained in general terms. An Appendix is included giving the exponential horn design criteria.

[REDACTED]

[REDACTED]

GEORGE C. MARSHALL SPACE FLIGHT CENTER

MTP-TEST-63-4

March 12, 1963

PERFORMANCE CHARACTERISTICS OF A LARGE FREE-FIELD
EXPONENTIAL HORN

By

Richard N. Tedrick

MEASURING AND INSTRUMENTATION BRANCH
TEST DIVISION

LIST OF ILLUSTRATIONS

Figure	Title	Page
1.	Exponential Horn Installation at Marshall Space Flight Center	8
2.	Low Frequency Cut-off of Horn as a Function of Temperature	9
3.	Side View of Horn Showing Interior Measurement Planes. . . .	10
4.	Internal Variations of Sound Pressure Level Along Centerline of Horn.	11
5.	Calculation and Measured Sound Pressure Levels Inside and in Front of Horn.	12
6.	End View of Horn Showing Measurement Radii.	13
7.	SPL Variations Across the Face of the Horn at 25 and 50 cps	14
8.	SPL Variations Across the Face of the Horn at 100 and 200 cps.	15
9.	SPL Variations Across the Face of the Horn at 400 and 800 cps.	16
10.	Measured Frequency Response at Various Locations in the Plane of the Mouth	17
11.	The Control Console of the Horn Installation.	18
12.	Electrical System Block Diagram	19
13.	Pneumatic System Block Diagram	20
A-1	Dimensions of Exponentially Expanded Horn	27

PRECEDING PAGE BLANK NOT FILMED

iv blank

GEORGE C. MARSHALL SPACE FLIGHT CENTER

MTP-TEST-63-4

PERFORMANCE CHARACTERISTICS OF A LARGE FREE-FIELD
EXPONENTIAL HORN

By

Richard N. Tedrick

SUMMARY

This report presents the characteristics of a large electro-pneumatic transducer and exponential horn system which was installed at Marshall Space Flight Center to simulate the rocket engine noise produced during a static test. The output of the system was found experimentally to be about 24 decibels lower than the SATURN S-I static tests.

Performance characteristics are presented showing the frequency response of the horn as a mechanical coupler into the atmosphere. The electrical, electronic and pneumatic control systems are explained in general terms. An Appendix is included giving the exponential horn design criteria.

INTRODUCTION

One of the malevolent by-products of the testing of today's large space vehicles is the high intensity sound generated by the rocket engines. This noise is capable of propagating several miles since it is mostly composed of low frequencies which attenuate relatively little. Then if, as often occurs, the prevailing meteorological conditions are right for refraction (bending) of the acoustic energy toward the earth, the sound pressure level at eight or ten miles from the test may actually be greater than the level measured just a few thousand feet away.

In order to protect the neighboring communities during tests of the Saturn space vehicle, the Test Division of Marshall Space Flight Center has instituted several programs to investigate the long-range propagation of sound. One of these involves the use of the exponential horn installation atop the 20 meter tower shown in Figure 1. Since the system is capable of sounding tones between 27 and 1000 cycles per second, the horn may be used to measure the attenuation of sound in the atmosphere as a function of frequency. Shaped random noise may also be "played" to approximate the acoustic output from rocket engines so that the acoustic effects of static firings under different meteorological conditions may be studied without either the risk or expense of such static tests.

DISCUSSION

The system basically consists of four electro-pneumatic transducers with an exponentially expanded coupler (horn). The transducers are Ling-Altec Model 6786 and they each electromagnetically modulate a 7097 liters per minute airflow operating at a pressure of 2.18 kilograms per square centimeter. With an electrical input of 75 watts each transducer is rated at approximately 2000 acoustic watts output. (This may be compared with the usual high-fidelity system which has an output of between 10 and 40 acoustic watts).

The horn, itself, is nearly 10 meters in length and is exponentially expanded to an exit diameter of 3.186 meters. This corresponds to a low frequency cut-off of 27.7 cycles per second at a virtual temperature of 20°C (68°F). The design criteria of the exponential horn are derived in the Appendix.

It was noted by the operators of the system that the horn and tower began to vibrate severely when the operating frequency was below thirty cycles per second. Upon investigation this was found to be the result of operating below the low frequency cut-off of the horn. Since it was found that this low-frequency cut-off was quite sharp, it was possible to study its variation with ambient air temperature. A theoretical relationship was derived (see Appendix) from the equation for the exponential horn. Several tests were made at various temperatures, and their results along with the calculated values are shown in Figure 2.

Tests were made of the sound pressure level variation within the horn itself. At four points along the centerline of the horn (see Figure 3) measurements were made at octave frequencies between 25 and 800 cps. The results

of these investigations are shown in Figure 4. The 25 cps signal which is below the cut-off of the horn is lower in sound pressure level at all stations along the centerline, while the 800 cps signal shows a slight reduction in level from the others at every position but the center of the horn mouth plane (plane D). One other notable characteristic of the curves is the nearly constant 3.5 db per meter loss along the horn centerline. The inverse square law appears not to apply in this case. This can be demonstrated theoretically by considering the expansion of the sound front within the horn.

The equation for the side of the exponentially-expanding horn (see Appendix Figure A-1) is in the general form

$$y = ae^{bx} \quad (1)$$

where a and b are experimentally-derived constants (see Appendix). The area (A) of the cross-section of a square horn is

$$\begin{aligned} A &= (2y)^2 \\ &= 4a^2e^{2bx} \end{aligned} \quad (2)$$

However, at the input to the horn ($x=0$), the cross-sectional area $A_0 = 4a^2$. Thus

$$A = A_0e^{2bx} \quad (3)$$

The sound pressure level (SPL) and power level (PWL) are related by the equation

$$SPL = PWL - 10 \log A \quad (4)$$

Therefore

$$\begin{aligned} SPL &= PWL - 10 \log A_0e^{2bx} \\ &= PWL - 10 \log A_0 - 10 \log e^{2bx} \end{aligned} \quad (5)$$

If one defines SPL_0 as the sound pressure level at the input to the horn ($x = 0$), then

$$SPL_0 = PWL - 10 \log A_0 \quad (6)$$

and, more generally,

$$\text{SPL} = \text{SPL}_0 - 20bx \log e - C \quad (7)$$

C is the constant in decibels to correct for the difference between the actual spherical wave segment and the assumed planar wave.

For the specific horn vehicle being considered (see Appendix) $b = 0.423$, $c = 9.49$ decibels and therefore

$$\text{SPL} = \text{SPL}_0 - 3.66 x - 9.49 \quad (8)$$

where x is the distance from the entrance to the horn in meters. As can be seen from Equation 8, the sound pressure level within the horn should be linear with distance from the throat.

It is interesting also to consider what happens just outside the horn, since it has been noted that the sound from such horns does not follow the classical inverse square law type of propagation loss. As mentioned before, the equation for the side of the horn is

$$y = ae^{bx} \quad (9)$$

Then

$$\frac{dy}{dx} = abe^{bx} = by \quad (10)$$

If, at the lip of the horn, the coordinates of the horn are (X_m, Y_m) and if it can be assumed that a portion of the sound wave front continues to travel along a line tangent to the horn lip, then a point along the edge of the forward-moving portion of the sound front would have the coordinates, $x = x_m + \Delta x$, $y = y_m + \Delta y$. However, if the angle included between the above mentioned tangent and the horn centerline is defined as θ , then

$$\tan \theta = \frac{dy}{dx} = by_m = \frac{\Delta y}{x - x_m} \quad (11)$$

and

$$\Delta y = (x - x_m) by_m \quad (12)$$

$$\begin{aligned} y &= y_m + \Delta y \\ &= y_m + (x - x_m) by_m \\ &= y_m [1 + b(x - x_m)] \end{aligned} \quad (13)$$

The sound pressure level at a point in front of the horn is (from Equations 4, 7 and 13) .

$$\text{SPL} = \text{SPL}_O - 3.66 X_m - 20 \log [1 + b(x-x_m)] - c \quad (14)$$

For the condition under which X is much greater than one, Equation 14 becomes

$$\text{SPL} = \text{SPL}_O - 3.66 X_m - 20 \log b - 20 \log (x-x_m) - c \quad (15)$$

If X is also much larger than X_m (in other words if the measuring point is in front of the horn several multiples of the horn length) , then

$$\text{SPL} = \text{SPL}_O - 3.66 X_m - 20 \log b - 20 \log x - c \quad (16)$$

The sound pressure level at the mouth of the horn SPL_m may be defined as

$$\text{SPL}_m = \text{SPL}_O - 3.66 X_m - 20 \log b - c.$$

Therefore

$$\text{SPL} = \text{SPL}_m - 20 \log x \quad (17)$$

This is the well-known inverse square law. Thus the limitations upon the application of the inverse square law can be seen. That rule may be considered to be useful only when the distance (x) from the source is much greater than the length of the horn itself.

In the case of the specific horn which is under consideration, Equation 14 becomes (when x is in meters)

$$\begin{aligned} \text{SPL} &= \text{PWL} - 10 \log (0.0298) - 10 \log (3.28)^2 - 3.66 (7.32) - 9.49 \\ &\quad - 20 \log [1 + 0.423(x-7.32)] \\ &= \text{PWL} - 19.8 - 20 \log [1 + 0.423(x-7.32)] \end{aligned} \quad (18)$$

When Equations 8 and 18 are plotted, a single smooth curve (Fig. 5) is obtained. The measured values taken within the horn and within one thousand feet of the horn have been added to the figure along with the inverse square law reference line which might be inferred from the far-field data.

Measurements of sound pressure level variations in the plane of the mouth of the horn (plane D) were also made (see Figure 6) at octave frequencies. The results of these measurements are presented in Figures 6 through 9. The sound pressure level variations across the face of the horn at 25 and 50 cycles per second are shown in Figure 7. The 25 cps curve shows the effect of being below the cut-off frequency in that it is six to ten decibels lower than the other curve. This means that there is from one quarter to one tenth as much energy being radiated at 25 as at 50 cps. Most or all of the remainder is going into the vibration mentioned above.

In Figures 8 and 9, the same type of presentation is made of the energy at 100, 200, 400 and 800 cps. At 200 cps a peak begins to show in the curve at the center of the horn mouth. This phenomenon increases with frequency until at 800 cps the wave front of the energy can be seen to even pull away from the edges and corners of the horn. This is due to the proportional decrease in wavelength as the frequency increases. In this case not more energy but less is imparted to the horn in the form of vibration. However, the efficiency of a horn which is too large for the wavefront is lower and the resulting sound pressure level output is less.

In Figure 10 the information from the previous three figures is summarized. The measured frequency response curves for various locations in the plane of the horn mouth are shown. The portions of the curves which lie between 50 and 400 cps appear to be relatively flat. This is, of course, indicative of the optimum frequency range of the horn system. It should be noted that the absolute sound pressure levels shown across the face and at interior planes were not taken at full power. This was done to protect the equipment and personnel during the test. However, none of the cut-off data nor frequency response curves should be materially altered by changes in amplitude.

At full power the output of the exponential horn installation is 151 decibels at six feet in front of the mouth of the horn along the centerline. In the field the sound pressure level is about 24 decibels below that measured during Saturn static tests. This means that while under most meteorological conditions the signal can be heard well above the ambient background noise level out to twelve to fifteen miles, it has only one sixteenth the damaging pressure of the Saturn test. Thus the horn can be sounded while several mobile monitoring stations are in the Huntsville area and the findings utilized to reschedule full-scale rocket tests to avoid periods of possible damage or annoyance which might result under adverse conditions.

The control console installation in the tower is shown in Figure 11. The electrical and electronic circuitry is quite simple. It consists of three audio oscillators and a random noise generator, any one of which (or each in turn) may be played through two power amplifiers into the electro-pneumatic transducers. (Figure 12). It has been determined that when there is an electrical signal across the transducers it is necessary to have the air flowing through them to keep the relatively delicate coils from overheating. Therefore, to keep a load across the output of each amplifier between tests, artificial loads were hand wound and are inserted in the circuit by relay action each time the signal is removed from the transducer. The length of time the transducer is activated is governed by a pre-set time delay circuit. By use of the stepping relay, it is possible to "play" a series of three pre-determined tones and random noise.

The azimuth of the horn is variable since the platform upon which it rests may be rotated 340°. (Because of the flair of the horn it is possible for the operator to direct sound out every azimuth). A reversible 220 volt, 3 phase, 40 horse power chain-drive motor turns the horn about 15 degrees per minute. This is controlled like the rest of the system from within the control room atop the tower.

The pneumatic system (Figure 13) consists of a diesel-powered compressor, a collection tank, a dome regulator controlled by a small manual regulator and several filters. Because of the high magnetic flux density (17,000 gauss), every particle of iron which may be generated within the system by the friction of moving parts or sucked in from the outside at the compressor eventually finds its way to the permanent magnets in the transducer. Since the extremely small tolerances between the magnet and moving coil do not leave much room for such accumulation before the coil is shorted, it has been necessary to filter out every impurity down to 40 microns in size.

ORIGINAL PAGE
BLACK AND WHITE PHOTOGRAPH

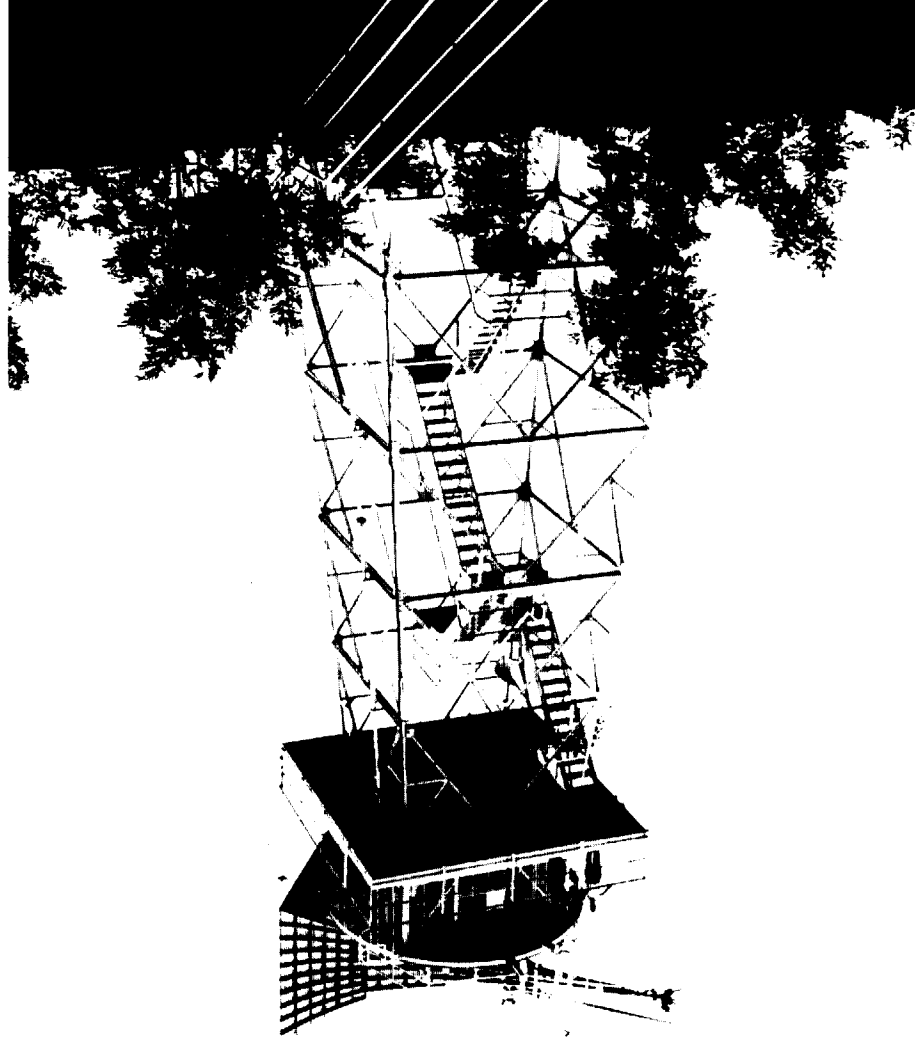


FIGURE 1. EXPONENTIAL HORN INSTALLATION AT MARSHALL SPACE FLIGHT CENTER

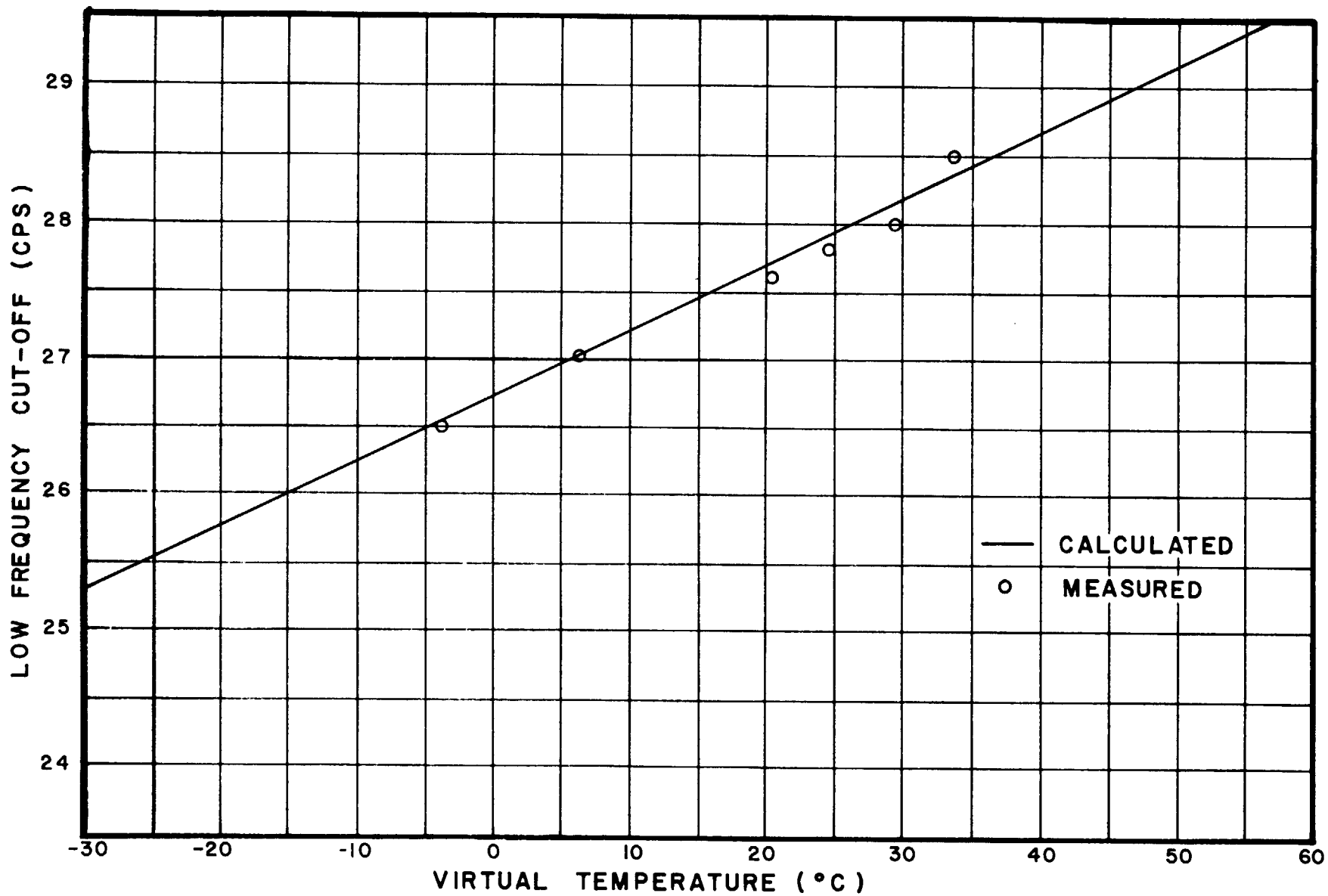


FIGURE 2. LOW FREQUENCY CUT-OFF OF HORN AS A FUNCTION OF TEMPERATURE

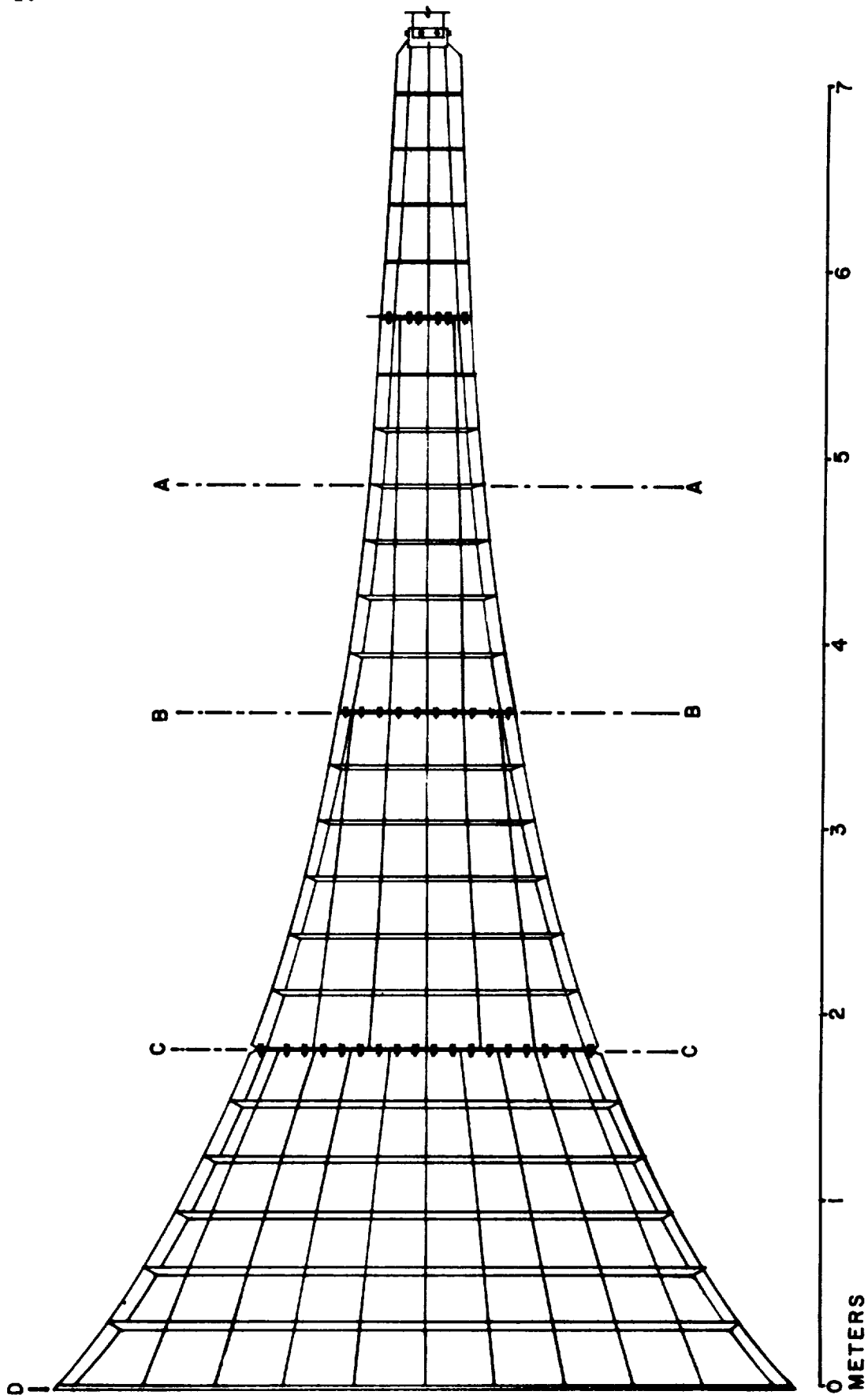


FIGURE 3. SIDE VIEW OF HORN SHOWING INTERIOR MEASUREMENT PLANES

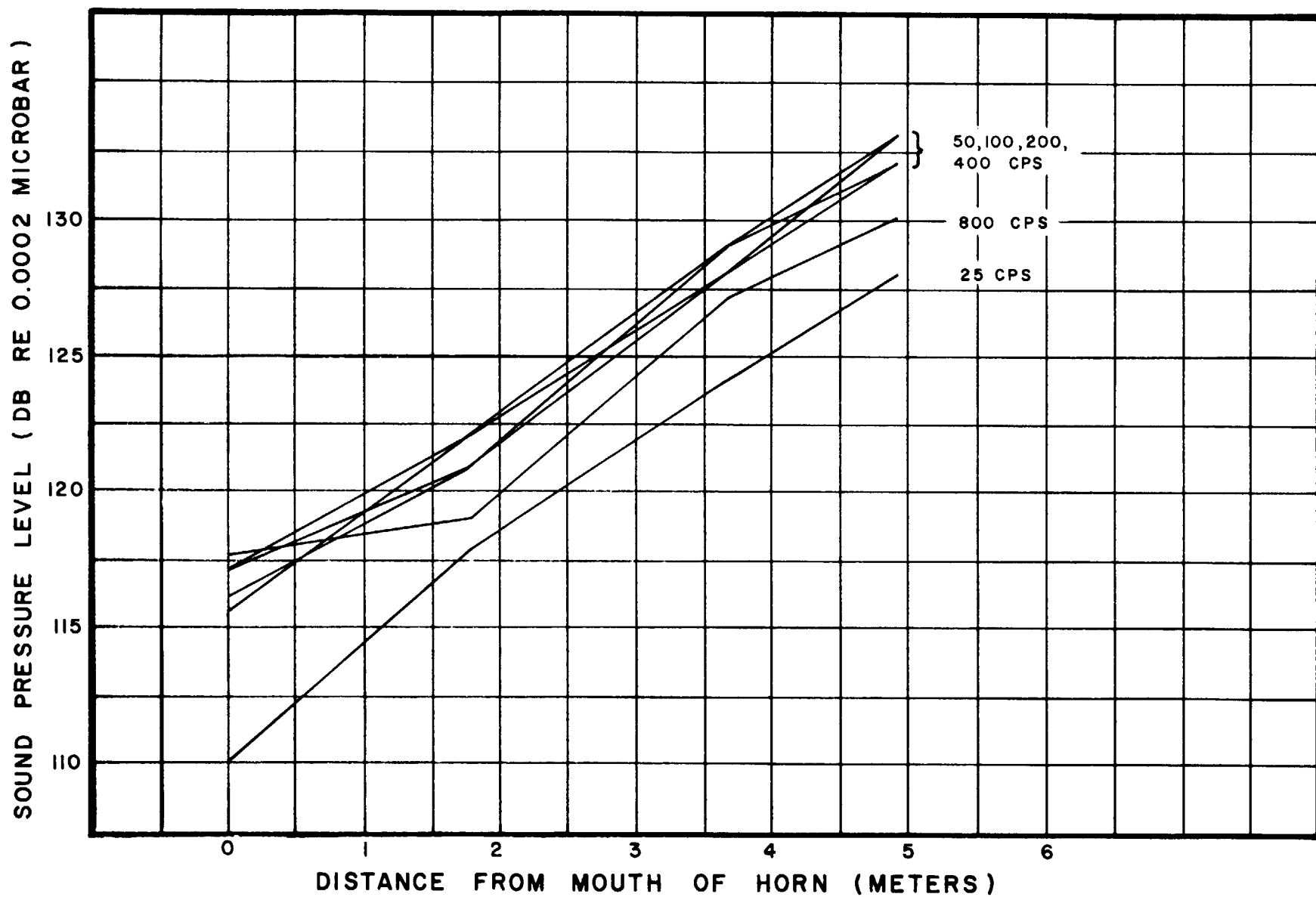


FIGURE 4. INTERNAL VARIATIONS OF SOUND PRESSURE LEVEL ALONG CENTERLINE OF HORN

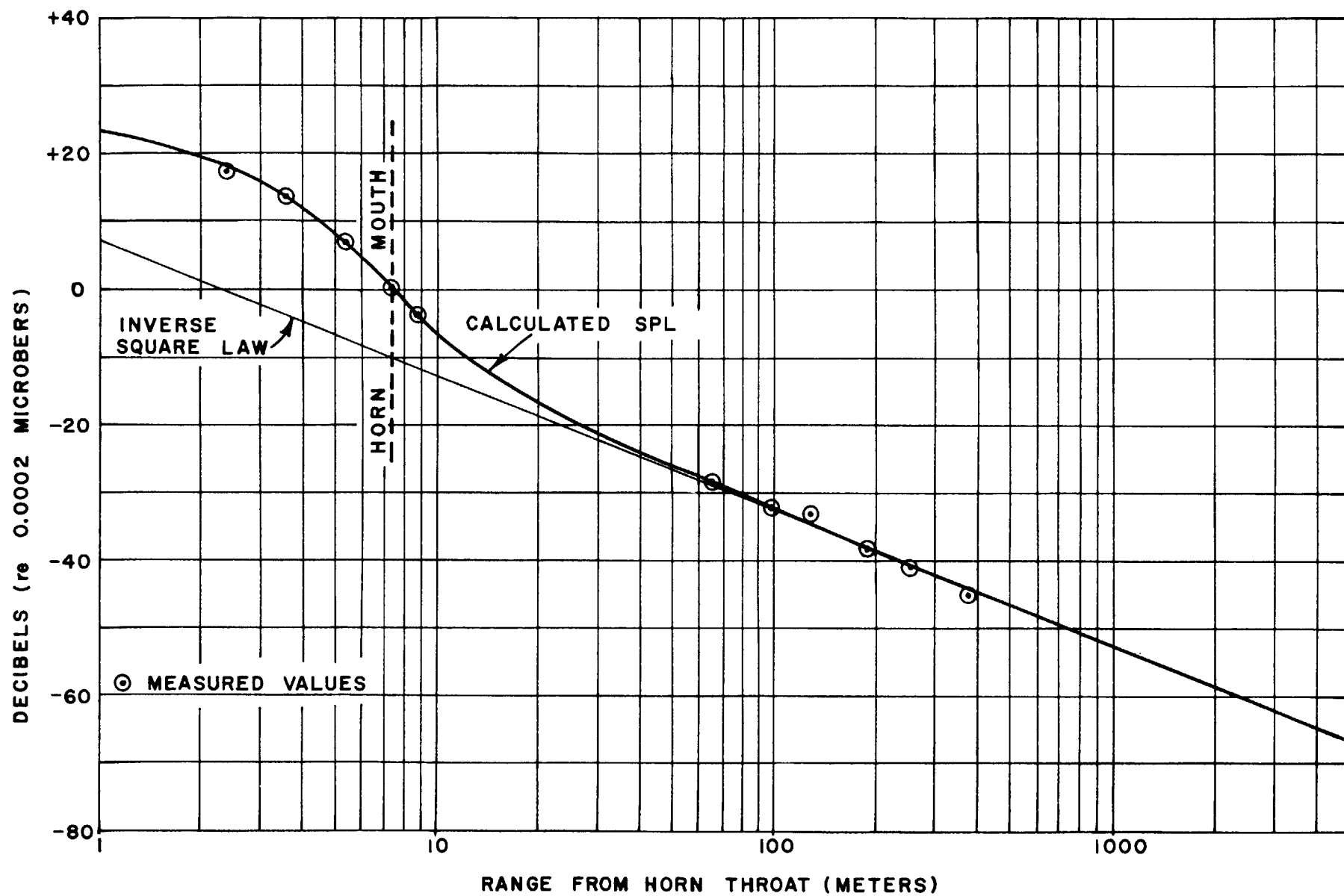


FIGURE 5. CALCULATION AND MEASURED SOUND PRESSURE LEVELS INSIDE AND IN FRONT OF HORN

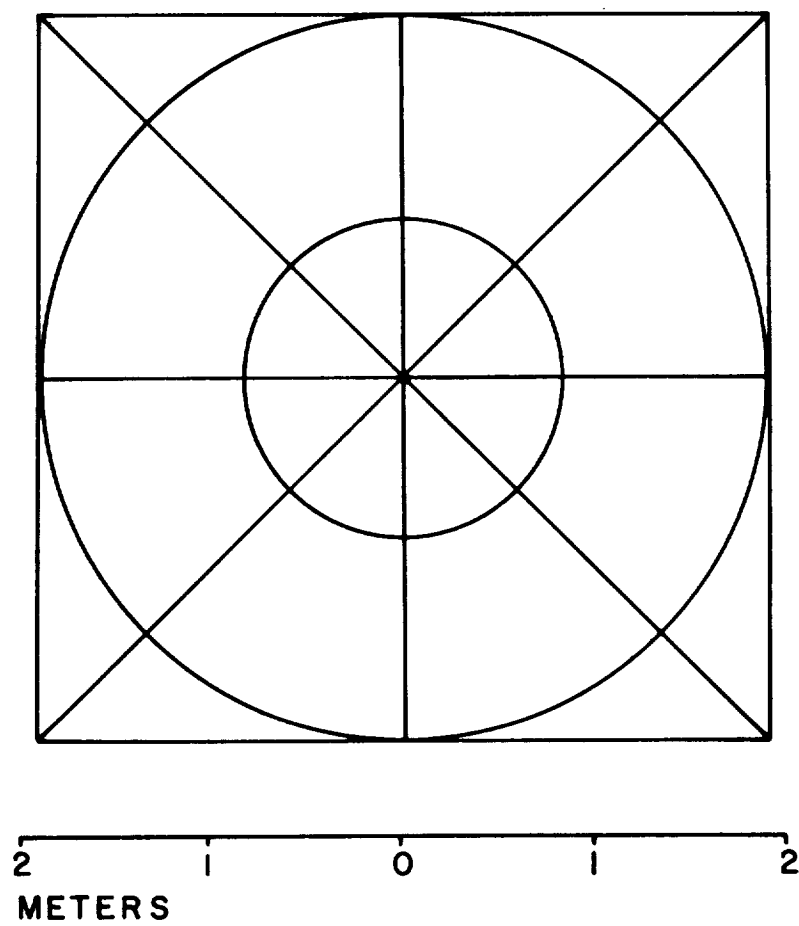


FIGURE 6. END VIEW OF HORN SHOWING MEASUREMENT RADII

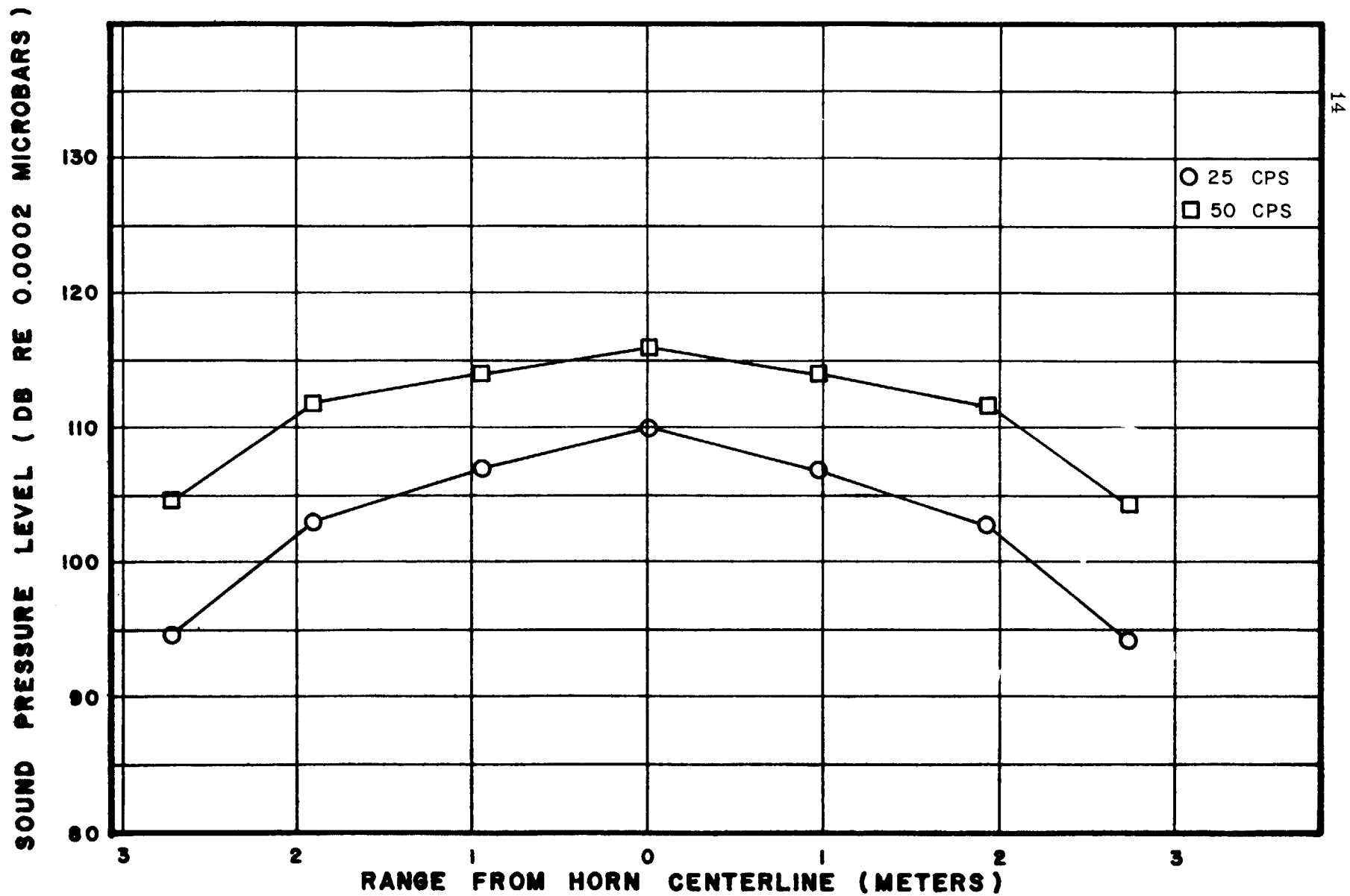


FIGURE 7. SPL VARIATIONS ACROSS THE FACE OF THE HORN AT 25 AND 50 CPS

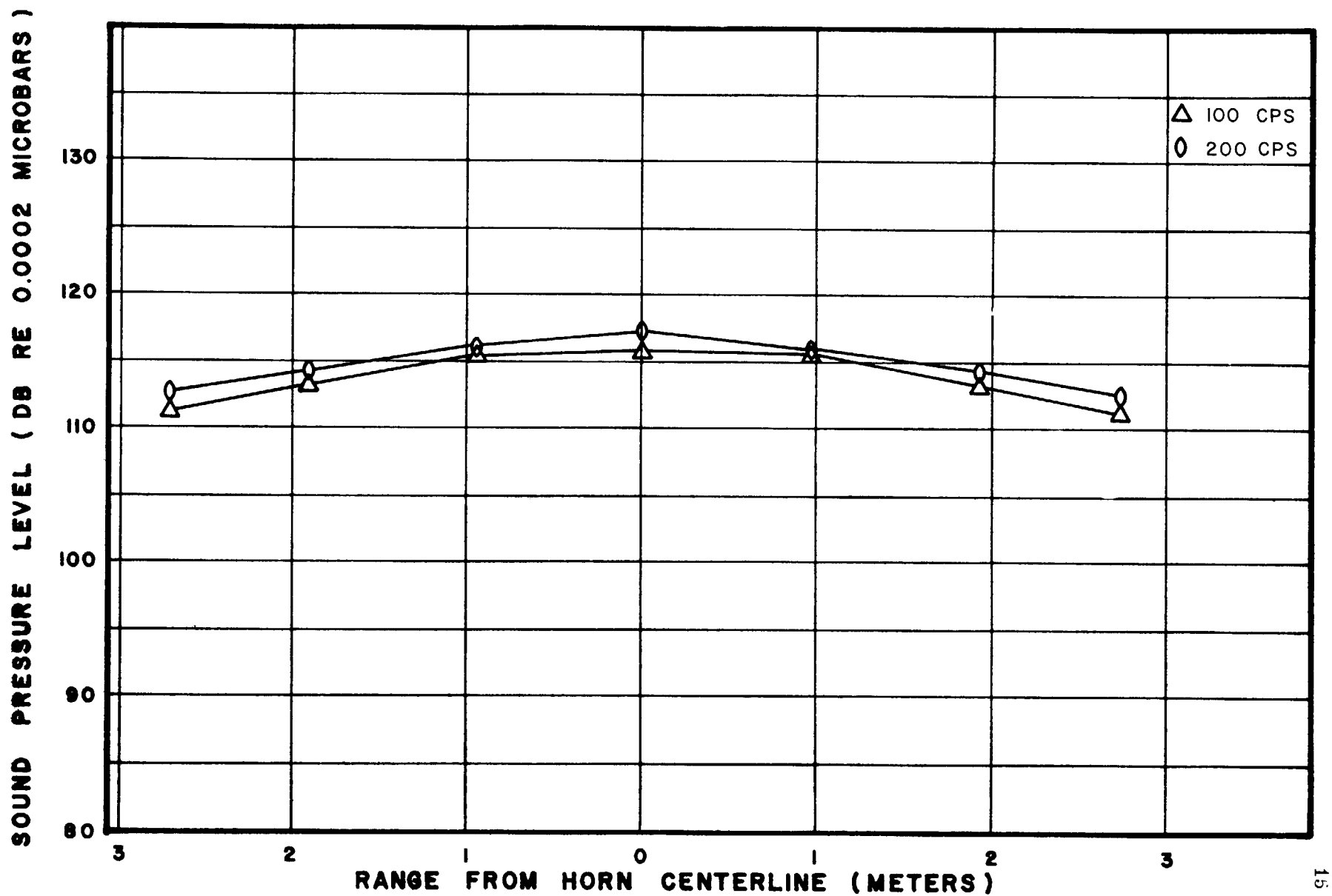


FIGURE 8. SPL VARIATIONS ACROSS THE FACE OF THE HORN AT 100 AND 200 CPS

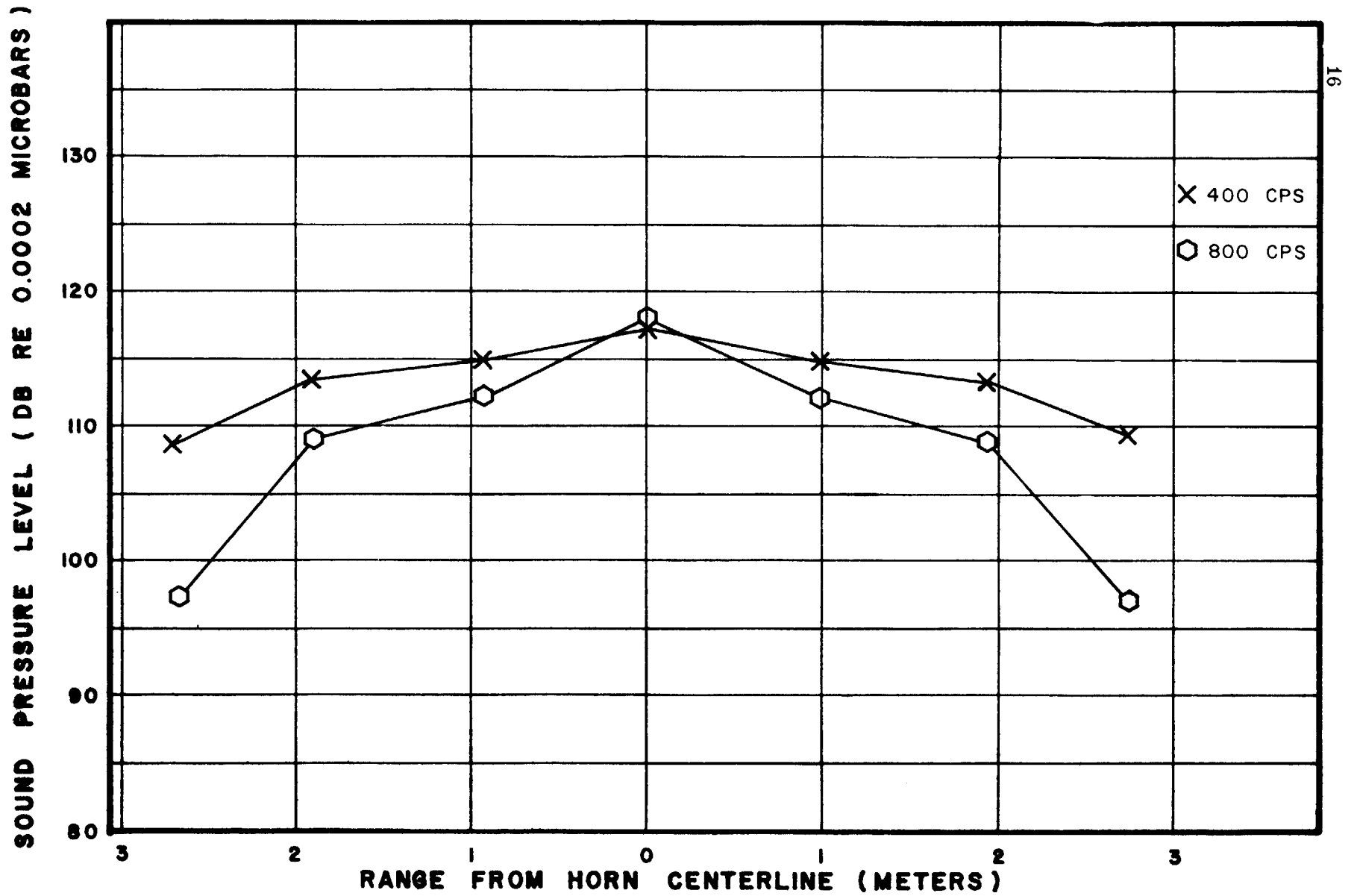


FIGURE 9. SPL VARIATIONS ACROSS THE FACE OF THE HORN AT 400 AND 800 CPS

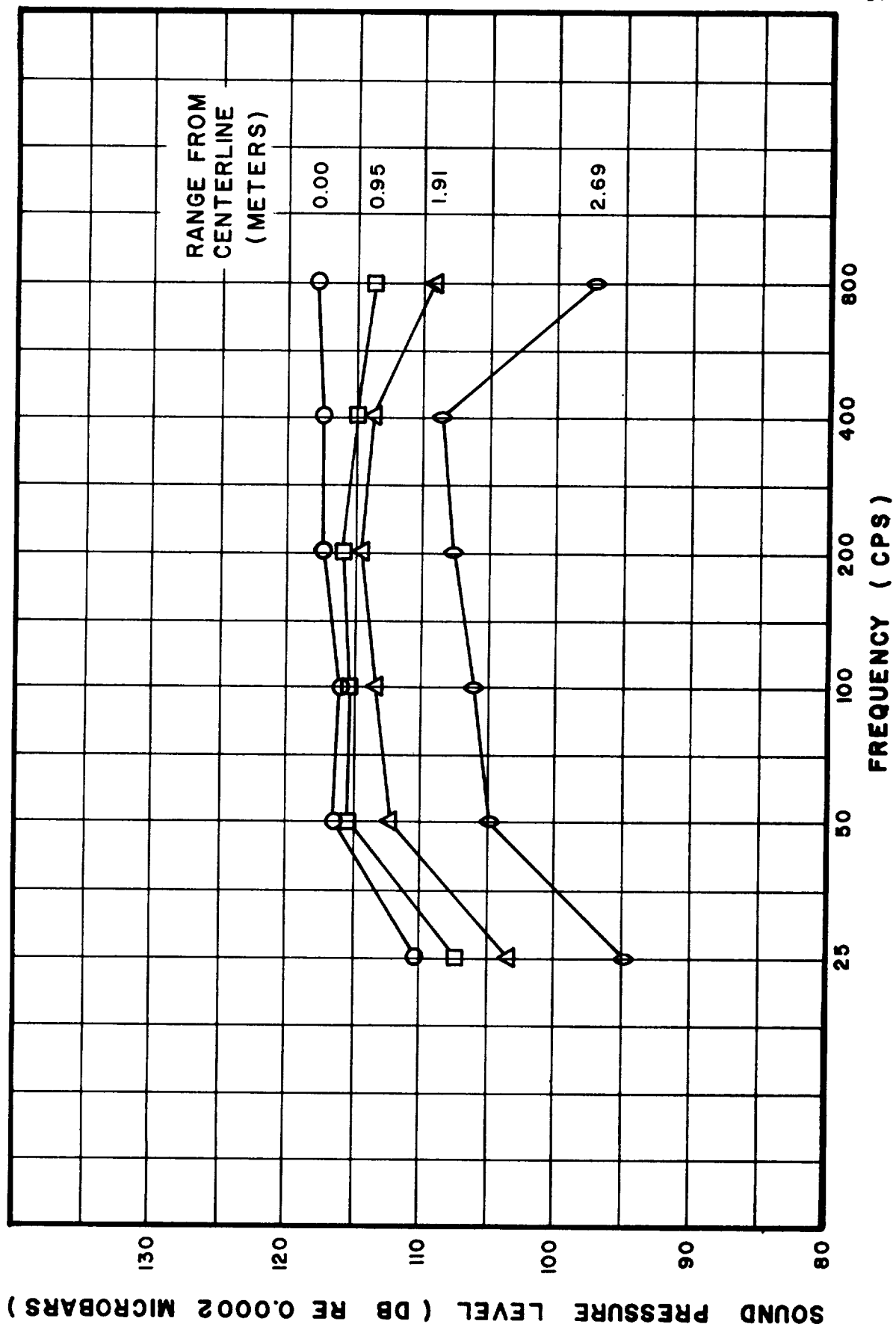


FIGURE 10. MEASURED FREQUENCY RESPONSE AT VARIOUS LOCATIONS IN THE PLANE OF THE MOUTH

ORIGINAL PAGE
BLACK AND WHITE PHOTOGRAPH



FIGURE 11. THE CONTROL CONSOLE OF THE HORN INSTALLATION

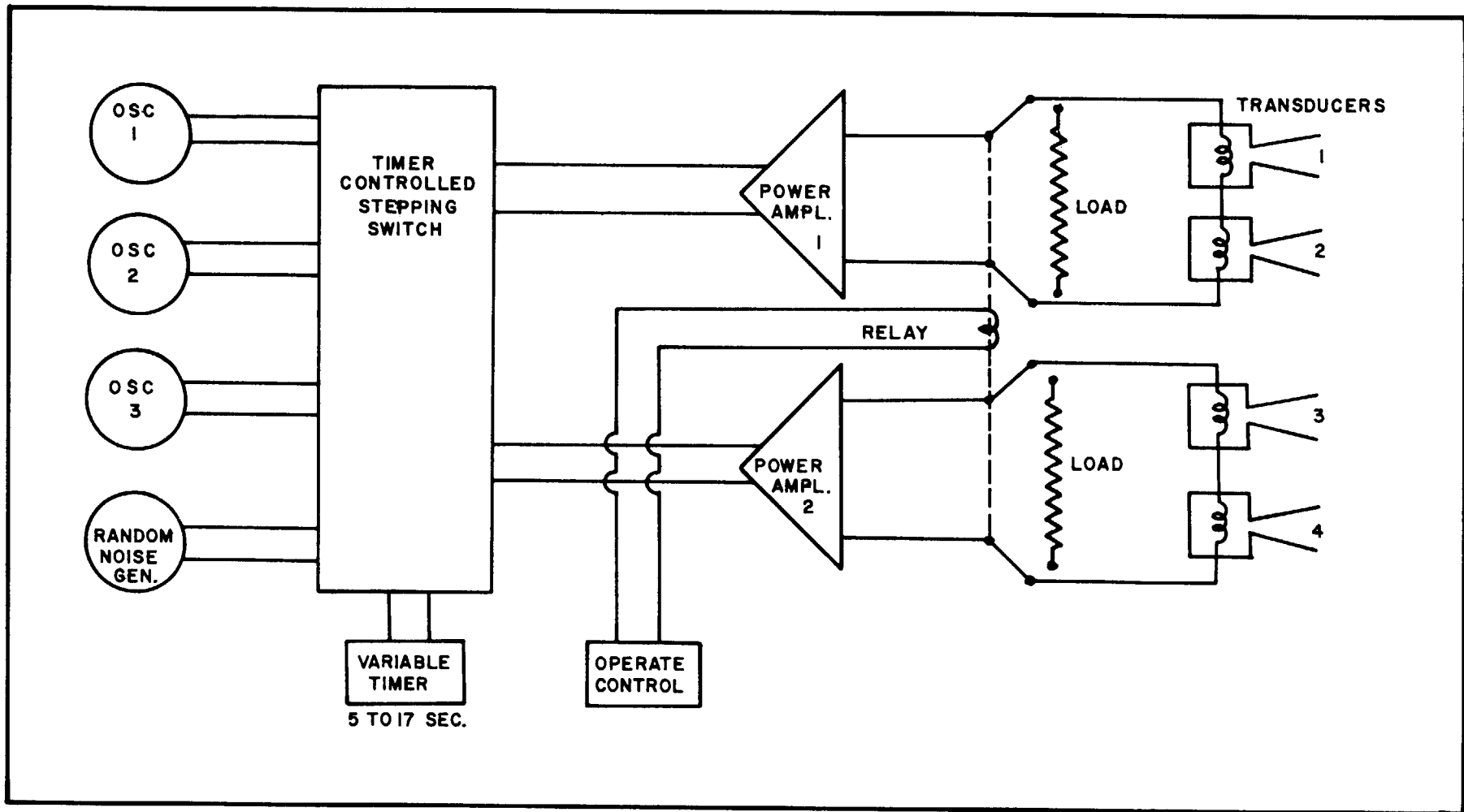


FIGURE 12. ELECTRICAL SYSTEM BLOCK DIAGRAM

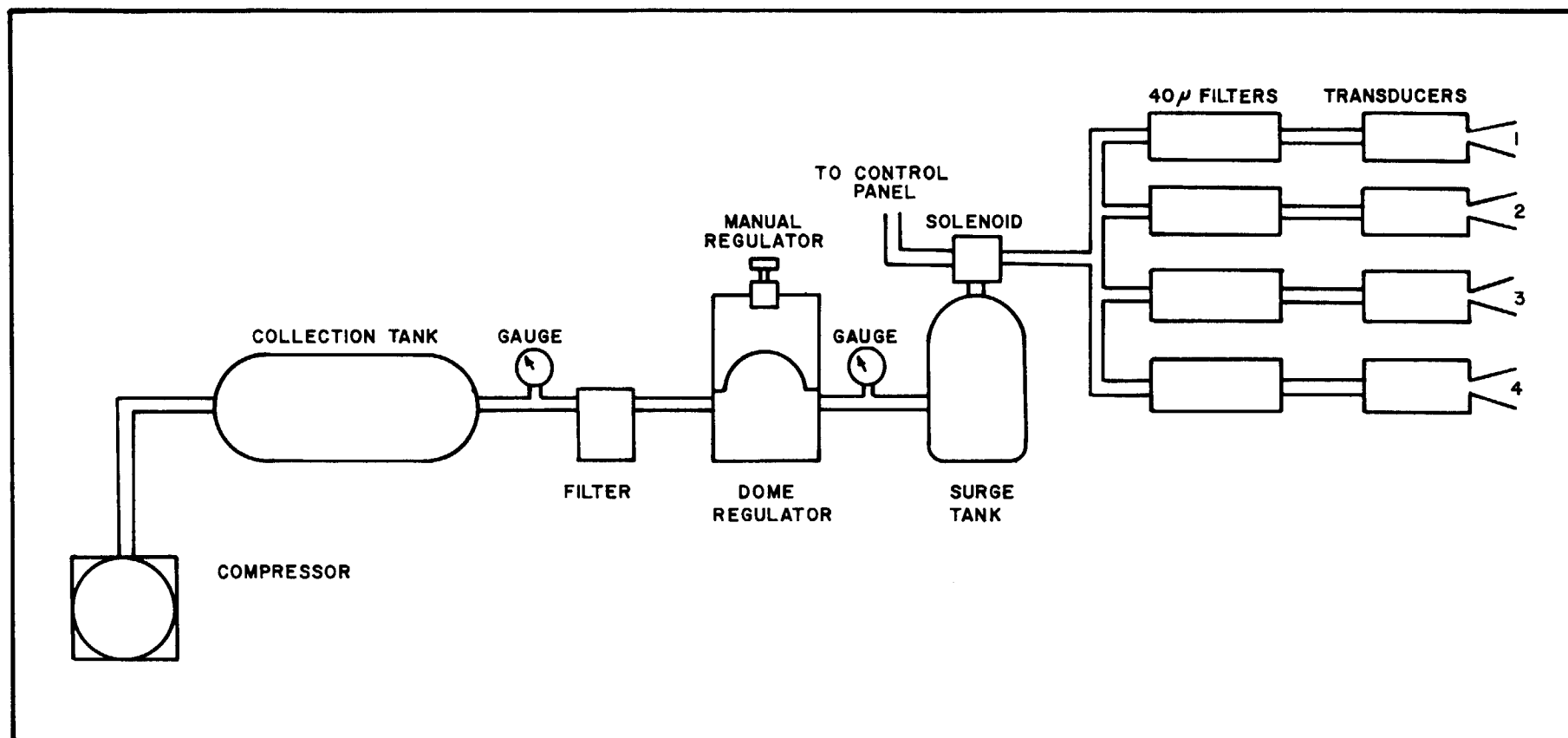


FIGURE 13. PNEUMATIC SYSTEM BLOCK DIAGRAM

APPENDIX A

CALCULATION OF HORN CRITERIA

1. Assume horn throat dimensions (square) of 17.27 centimeters ($D_o = 17.27$ cm)
2. Assume an exit cutoff frequency of 30 cycles per second ($f_c = 30$ cps)
3. Assume an atmospheric temperature of 20°C. This results in a velocity of sound of 343.7 meters per second ($V_s = 343.7$ mps)
4. Wave length at cutoff (λ) is

$$\lambda = \frac{V_s}{f_c} = \frac{343.7}{30} = 11.46 \text{ meters}$$

5. Exit side (D_c) should be approximately

$$D_c = \frac{\lambda}{3} = \frac{11.46}{3} = 3.82 \text{ meters}$$

6. Maximum exponential flaring constant (m) is (Ref. 1)

$$m = \frac{10.5}{\lambda} = \frac{10.5}{11.46} = 0.916$$

7. Length of horn (L) in meters is

$$L = \frac{4.605}{m} \log \left(\frac{D_c}{D_o} \right)$$

$$= 5.03 \log (22.119)$$

$$= 6.77 \text{ meters}$$

8. For structural reasons, assume the length to be 7.31 meters instead of 6.77 meters. Then the flaring constant would be

$$\begin{aligned} m' &= \frac{4.605}{7.31} \log \frac{D_c}{D_o} \\ &= 0.630 \log (22.119) \\ &= 0.846 \end{aligned}$$

9. The length of the side at X distance from throat = $y = D_o \epsilon^{mx/2}$

$$= (0.1727) (2.718)^{0.423x}$$

10. Since $m' = \frac{10.5}{\lambda}$ and $\lambda = \frac{V_s}{f_c}$

$$f_c = \frac{V_s m'}{10.5}$$

11. However $V_s = 20.06 T^{-2}$ where T is the virtual temperature in degrees Kelvin ($^{\circ}K$). Therefore

$$\begin{aligned} f_c &= \frac{20.06 m' T^{-2}}{10.5} \\ &= 1.62 T^{-2} \end{aligned}$$

Relationships 9 and 11 allow the calculation of the dimensions of the horn configuration itself and the cut-off frequency of the horn. Table A-1 lists the x distance from the throat and the corresponding side length y. Figure A-1 presents the same data graphically. The calculated values of the cut-off frequency are plotted against measurements in the main body of the report.

TABLE A-1
CALCULATED HORN DIMENSIONS

Item No.	X Distance From Horn Throat (cm)	$y = D_o \epsilon^{mx/2}$	Width of Horn Section (cm)
1	15.24	$y^1 = (17.27)(2.718)^{0.0645} = (17.27)(1.0666) =$	18.42
2	30.48	$y^2 = (17.27)(2.718)^{0.1289} = (17.27)(1.1365) =$	19.63
3	45.72	$y^3 = (17.27)(2.718)^{0.1934} = (17.27)(1.2133) =$	20.96
4	60.96	$y^4 = (17.27)(2.718)^{0.2597} = (17.27)(1.2942) =$	22.35
5	76.20	$y^5 = (17.27)(2.718)^{0.3224} = (17.27)(1.3804) =$	23.84
6	91.44	$y^6 = (17.27)(2.718)^{0.3868} = (17.27)(1.4723) =$	25.43
7	106.68	$y^7 = (17.27)(2.718)^{0.4513} = (17.27)(1.5703) =$	27.12
8	121.92	$y^8 = (17.27)(2.718)^{0.5158} = (17.27)(1.6750) =$	28.93
9	137.16	$y^9 = (17.27)(2.718)^{0.5803} = (17.27)(1.7865) =$	30.86
10	152.40	$y^{10} = (17.27)(2.718)^{0.6447} = (17.27)(1.9054) =$	32.91
11	167.64	$y^{11} = (17.27)(2.718)^{0.7092} = (17.27)(2.0324) =$	35.10
12	182.88	$y^{12} = (17.27)(2.718)^{0.7737} = (17.27)(2.1678) =$	37.44

TABLE A-1 (Cont'd)

Item No.	X Distance From Horn Throat (cm)	$y = D_o \epsilon^{mx/2}$	Width of Horn Section (cm)
13	198.12	$y^{13} = (17.27)(2.718)^{0.8382} = (17.27)(2.3122) =$	39.94
14	213.36	$y^{14} = (17.27)(2.718)^{0.9026} = (17.27)(2.4660) =$	42.59
15	228.60	$y^{15} = (17.27)(2.718)^{0.9671} = (17.27)(2.6303) =$	45.43
16	243.84	$y^{16} = (17.27)(2.718)^{1.0316} = (17.27)(2.8056) =$	48.46
17	259.08	$y^{17} = (17.27)(2.718)^{1.0961} = (17.27)(2.9925) =$	51.69
18	274.32	$y^{18} = (17.27)(2.718)^{1.1605} = (17.27)(3.1915) =$	55.12
19	289.56	$y^{19} = (17.27)(2.718)^{1.2250} = (17.27)(3.4042) =$	58.80
20	304.80	$y^{20} = (17.27)(2.718)^{1.2895} = (17.27)(3.6310) =$	62.71
21	320.04	$y^{21} = (17.27)(2.718)^{1.3540} = (17.27)(3.8729) =$	66.89
22	335.28	$y^{22} = (17.27)(2.718)^{1.4184} = (17.27)(4.1205) =$	71.17
23	350.52	$y^{23} = (17.27)(2.718)^{1.4829} = (17.27)(4.4057) =$	76.09
24	265.76	$y^{24} = (17.27)(2.718)^{1.5474} = (17.27)(4.6993) =$	81.17

TABLE A-1 (Cont'd)

Item No.	X Distance From Horn Throat (cm)	$y = D_o \epsilon^{mx/2}$	Width of Horn Section (cm)
25	381.00	$y^{25} = (17.27)(2.718)^{1.6119} = (17.27)(5.0123) =$	86.57
26	396.24	$y^{26} = (17.27)(2.718)^{1.6763} = (17.27)(5.3458) =$	92.33
27	411.49	$y^{27} = (17.27)(2.718)^{1.7408} = (17.27)(5.7019) =$	98.48
28	426.72	$y^{28} = (17.27)(2.718)^{1.8053} = (17.27)(6.0818) =$	105.04
29	441.72	$y^{29} = (17.27)(2.718)^{1.8698} = (17.27)(6.4870) =$	112.04
30	457.20	$y^{30} = (17.27)(2.718)^{1.9342} = (17.27)(6.9186) =$	119.50
31	472.45	$y^{31} = (17.27)(2.718)^{1.9987} = (17.27)(7.3795) =$	127.46
32	487.68	$y^{32} = (17.27)(2.718)^{2.0632} = (17.27)(7.8712) =$	135.95
33	502.93	$y^{33} = (17.27)(2.718)^{2.1277} = (17.27)(8.3956) =$	145.01
34	518.16	$y^{34} = (17.27)(2.718)^{2.1921} = (17.27)(8.9540) =$	154.65
35	533.41	$y^{35} = (17.27)(2.718)^{2.2566} = (17.27)(9.5507) =$	164.96
36	548.64	$y^{36} = (17.27)(2.718)^{2.3211} = (17.27)(10.1872) =$	175.95

TABLE A-1 (Cont'd)

Item No.	X Distance From Horn Throat (cm)	$y = D_0 \epsilon^{mx/2}$	Width of Horn Section (cm)
37	563.89	$y^{37} = (17.27)(2.718)^{2.3856} = (17.27)(10.8110) =$	186.73
38	579.37	$y^{38} = (17.27)(2.718)^{2.4500} = (17.27)(11.5880) =$	200.15
39	594.37	$y^{39} = (17.27)(2.718)^{2.5145} = (17.27)(12.3608) =$	213.50
40	609.60	$y^{40} = (17.27)(2.718)^{2.5790} = (17.27)(13.1839) =$	227.71
41	624.85	$y^{41} = (17.27)(2.718)^{2.6435} = (17.27)(14.0623) =$	242.88
42	640.08	$y^{42} = (17.27)(2.718)^{2.7079} = (17.27)(14.9977) =$	259.04
43	655.33	$y^{43} = (17.27)(2.718)^{2.7724} = (17.27)(15.9974) =$	276.31
44	670.56	$y^{44} = (17.27)(2.718)^{2.8369} = (17.27)(17.0630) =$	294.71
45	685.81	$y^{45} = (17.27)(2.718)^{2.9014} = (17.27)(18.1996) =$	314.34
46	701.04	$y^{46} = (17.27)(2.718)^{2.9658} = (17.27)(19.4105) =$	335.26
47	716.29	$y^{47} = (17.27)(2.718)^{3.0303} = (17.27)(20.7032) =$	357.59
48	731.52	$y^{48} = (17.27)(2.718)^{3.0948} = (17.27)(22.0831) =$	381.42

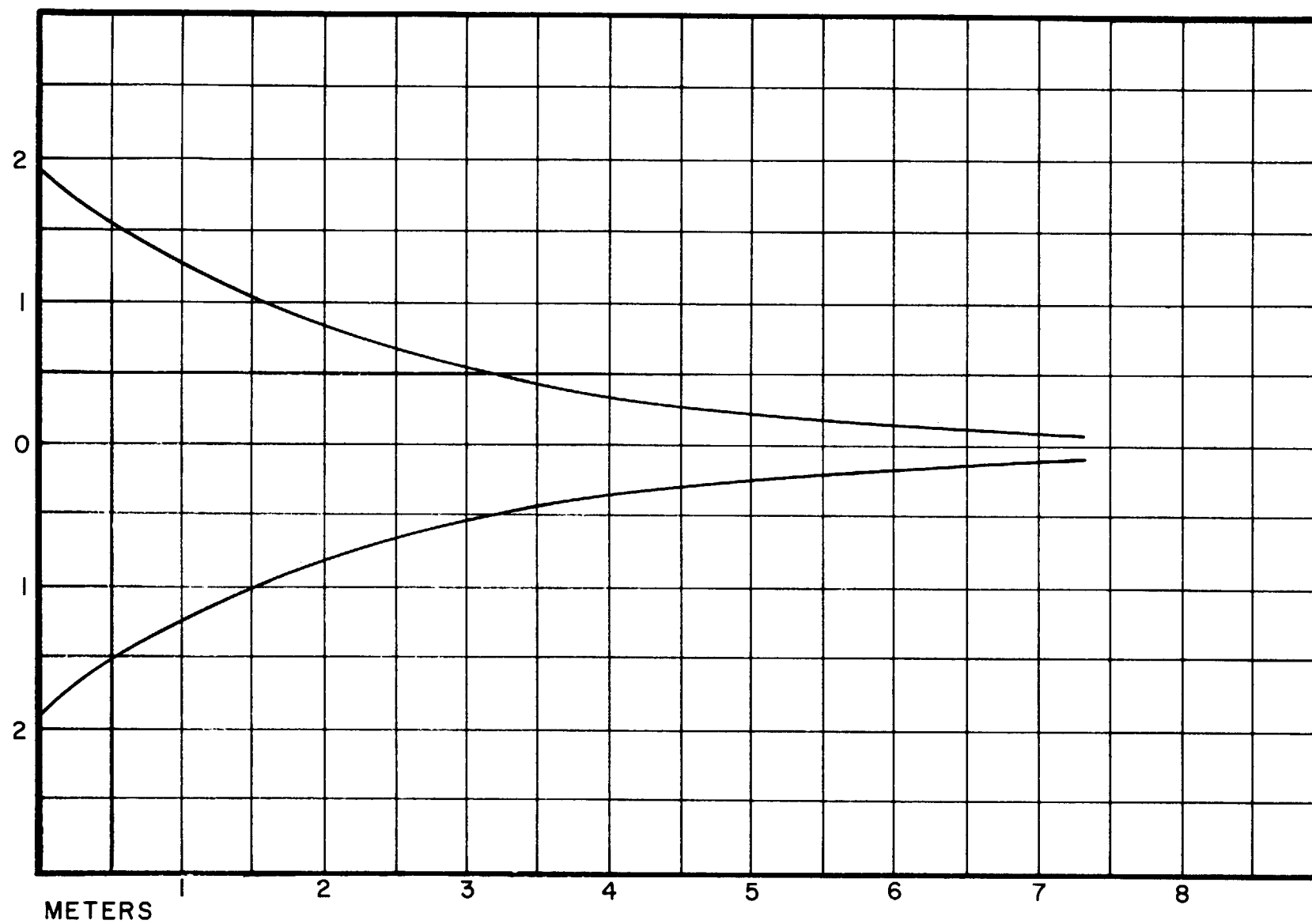


FIGURE A-1. DIMENSIONS OF EXPONENTIALLY EXPANDED HORN

REFERENCE

1. Ling-Altec, Inc., "Calculation of Horn Dimensions," Instructions furnished with transducers, 1962.

APPROVAL

PERFORMANCE CHARACTERISTICS OF A LARGE FREE-FIELD
EXPONENTIAL HORN

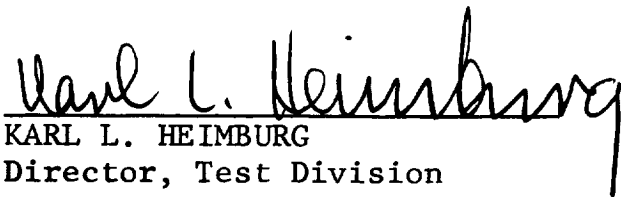
By

Richard N. Tedrick

The information in this report has been reviewed for security classification. Review of any information concerning Department of Defense or Atomic Energy Commission programs has been made by the MSFC Security Classification Officer. This report, in its entirety, has been determined to be unclassified.

C. C. THORNTON

Chief, Special Projects Unit
Components Instrumentation Section
Measuring and Instrumentation Branch

KARL L. HEIMBURG

Director, Test Division

DISTRIBUTION

INTERNAL

M-DIR von Braun	M-FPO-DIR Doelle
M-DEP-R D Rees	M-SAT-DIR Lange
M-AERO-DIR Geissler	M-MICH Constan
M-AERO-DEP Hoelker	M-LOC-DIR Debus
M-AERO-PS Jean	M-LOC-MQ Zeiler
M-AERO-A Dahm	M-LOC-E Sandler Williams
M-AERO-G Vaughan	M-LOC-C Moser
M-AERO-D Horn	M-LOC-M Gorman
M-AERO-E Holderer	M-LOC-TS Knothe
M-AERO-F Speer	M-LOC-D Poppel
M-ASTR-DIR Haeussermann	M-LOC-DS Brewster
M-ASTR-I Hoberg	M-LOC-ED Hershey (4)

INTERNAL DISTRIBUTION (Cont'd)

M-ASTR-DEP Bell	M-LOC-EM Wilkinson (4)
M-COMP-DIR Hoelzer	M-LOC-F Dodd Kavanaugh Deese
M-COMP-R Moore Felder	M-LOC-H Petrone (4)
M-LOC-OA Library (5)	M-LOC-SA Clark Abercrombie
M-L M-DIR Koers	M-LOC-ET White (10)
M-P VE-DIR Mrazek	M-LOC-GSE Stimson
M-P VE-DEP Weidner	M-HME-P
M-P VE-TSC Burrows	M-MS-H
M-P VE-SD Showers Farrow Gassaway (10)	M-MS-IPL (8)
M-QUAL-DIR Grau	M-MS-IP
M-RP-DIR Stuhlinger	M-PAT
M-TEST-DIR Heimburg	M-TEST-M Sieber
	M-TEST-TS Reisig
	M-REL Schulze

INTERNAL DISTRIBUTION (Cont'd)

M-PIO
Slattery

M-TEST-MC
Blake
Thornton (40)

DISTRIBUTION

EXTERNAL

ORDXM-OTL

Technical Library, AOMC (5)

Jet Propulsion Laboratory, CCMTA
H. Levy

Jet Propulsion Laboratory
4800 Oak Grove Drive
Pasadena 2, California
W. Pickering, DIR (4)

Director, Office of Manned Space Flight (3)
National Aeronautics and Space Administration
Washington 25, D. C.

Langley Research Center
National Aeronautics and Space Administration
Langley Field, Hampton, Virginia
Director (2)
Mr. H. H. Hubbard, Chief, Acoustics Branch

Director, Goddard Space Flight Center (2)
Greenbelt, Maryland

Director, Ames Research Center (2)
National Aeronautics and Space Administration
Moffett Field, California

EXTERNAL DISTRIBUTION (Cont'd)

Lewis Research Center
National Aeronautics and Space Administration
21000 Bookpark Road
Cleveland 35, Ohio
Director (2)
Technical Information Division (2)

Engineer in Charge (2)
Wallops Station
National Aeronautics and Space Administration

Director, Manned Spacecraft Center (2)
Post Office Box 1537
Houston, Texas

Pacific Missile Range (2)
Technical Library

Patrick Air Force Base (2)
Technical Library

White Sands Proving Ground (2)
Technical Library

Commander, AF Missile Test Center
Patrick AFB, Fla.,
ATTN: Tech Info and Intelligence Office, MIGRY

Hq. 6570 Aero Space Medical Research
Aero Space Division, AFSC
Wright Patterson AFB
Dayton, Ohio
Von Gierke (2)
Cole (2)

Scientific and Technical Information Facility (2)
ATTN: NASA Representative (S-AK/RKT)
P. O. Box 5700
Bethesda, Maryland

